

First results from the Very Small Array – IV. Cosmological parameter estimation

Jose Alberto Rubiño-Martin¹, Rafael Rebolo^{1,2}, Pedro Carreira³, †, Kieran Cleary³, Rod D. Davies³, Richard J. Davis³, Clive Dickinson³, Keith Grainge⁴, Carlos M. Gutiérrez¹, Michael P. Hobson⁴, Michael E. Jones⁴, Rüdiger Kneissl⁴, Anthony Lasenby⁴, Klaus Maisinger⁴, Carolina Ödman⁴, Guy G. Pooley⁴, Pedro J. Sosa Molina¹, Ben Rusholme^{4,*}, Richard D.E. Saunders⁴, Richard Savage⁴, Paul F. Scott⁴, Anže Slosar⁴, Angela C. Taylor⁴, David Titterington⁴, Elizabeth Waldram⁴, Robert A. Watson^{3,†} and Althea Wilkinson³

¹*Instituto de Astrofísica de Canarias, 38200 La Laguna, Tenerife, Canary Islands*

²*Consejo Superior de Investigaciones Científicas, Spain*

³*Jodrell Bank Observatory, University of Manchester, UK*

⁴*Astrophysics Group, Cavendish Laboratory, University of Cambridge, UK*

†*Present address: Instituto de Astrofísica de Canarias*

**Present address: Stanford University, Palo Alto, CA, USA*

Accepted —; received —; in original form 26 October 2018

ABSTRACT

We investigate the constraints on basic cosmological parameters set by the first compact-configuration observations of the Very Small Array (VSA), and other cosmological data sets, in the standard inflationary Λ CDM model. Using the weak priors $40 < H_0 < 90 \text{ km s}^{-1} \text{ Mpc}^{-1}$ and $0 < \tau < 0.5$, we find that the VSA and COBE-DMR data alone produce the constraints $\Omega_{\text{tot}} = 1.03_{-0.12}^{+0.12}$, $\Omega_b h^2 = 0.029_{-0.009}^{+0.009}$, $\Omega_{\text{cdm}} h^2 = 0.13_{-0.05}^{+0.08}$ and $n_s = 1.04_{-0.08}^{+0.11}$ at the 68 per cent confidence level. Adding in the type Ia supernovae constraints, we additionally find $\Omega_m = 0.32_{-0.06}^{+0.09}$ and $\Omega_\Lambda = 0.71_{-0.07}^{+0.07}$. These constraints are consistent with those found by the BOOMERanG, DASI and MAXIMA experiments. We also find that, by combining all these CMB experiments and assuming the HST key project limits for H_0 (for which the X-ray plus Sunyaev–Zel’dovich route gives a similar result), we obtain the tight constraints $\Omega_m = 0.28_{-0.07}^{+0.14}$ and $\Omega_\Lambda = 0.72_{-0.13}^{+0.07}$, which are consistent with, but independent of, those obtained using the supernovae data.

Key words: cosmology: observations – cosmic microwave background

1 INTRODUCTION

One of the central aims of cosmology is to determine the values of the fundamental cosmological parameters that describe our Universe. A unique opportunity to achieve this goal is provided by the observation of anisotropies in the cosmic microwave background (CMB) radiation. By comparing such observations with the predictions of our current theories of structure formation and the evolution of the Universe, we may place constraints on the cosmological parameters that appear in these models.

The currently most favoured theoretical model for de-

scribing our Universe is based on the idea of inflation (?), which provides a natural mechanism for producing initial density fluctuations described by a power-law spectrum with a slope close to unity. The simplest versions of inflation also predict the Universe to be spatially flat. The initial spectrum of adiabatic density fluctuations is modulated through acoustic oscillations in the plasma phase prior to recombination and the resulting inhomogeneities are then imprinted as anisotropies in the CMB. In the basic inflationary scenario, the CMB temperature anisotropies are predicted to follow a multivariate Gaussian distribution, and so may be com-

pletely described in terms of their angular power spectrum. Moreover, the acoustic oscillations in the plasma phase lead to a characteristic series of harmonic peaks in the power spectrum, which are a robust indicator of the existence of fluctuations on super-horizon scales.

Although the presence of acoustic peaks in the CMB power spectrum is a generic prediction of inflationary models, detailed features of the power spectrum, such as the relative positions and heights of the peaks, depend strongly on a wide range of cosmological parameters, see e.g. ?. Indeed, this sensitivity to the parameters is the reason why observations of the CMB provide such a powerful means of constraining theoretical models.

Thus measurement of the CMB power spectrum is a major goal of observational cosmology and numerous experiments have provided estimates of the spectrum on a range of angular scales. It is only recently, however, that observations by the BOOMERanG (?), DASI (?) and MAXIMA (?) experiments have provided measurements of the CMB power spectrum with sufficient accuracy over a wide range of scales to allow tight constraints to be placed on a wide range of cosmological parameters (see, for example, ?). This parameter estimation process is performed by comparing the observed band-powers with a wide range of theoretical power spectra corresponding to different sets of values of the cosmological parameters, which can be accurately calculated using the CMBFAST (?) or CAMB (?) software packages. The comparison of the observed and predicted power spectrum is usually carried out in a Bayesian context by evaluating the likelihood function of the data as a function of the cosmological parameters.

In this paper we perform this parameter estimation process using, as the main CMB datasets, the flat band-power estimates of the CMB power spectrum measured by the Very Small Array (VSA) in its compact configuration, which has been described in the sequence of earlier papers ?, ? and ? (Papers I, II and III), and the COBE-DMR band-powers for low- ℓ normalisation. We also combine the VSA data with other recent CMB experiments, and constraints from the HST Key Project on H_0 and observations of type Ia supernovae, to tighten further the constraints on the cosmological parameters. Two different methods are used to perform the parameter estimation procedure. First, we employ the traditional technique of evaluating the likelihood function on a large grid in parameter space. Second, we consider a more flexible approach in which the likelihood function is explored by Markov-Chain Monte Carlo (MCMC) sampling. The latter method has a great potential in terms of expanding the dimension of the parameter set which can be investigated. Here we use it to demonstrate the robustness of the results from the standard grid approach and also to provide a novel visualisation of the range of uncertainty in our parameter estimates.

2 MODELS, PARAMETER SPACE AND METHODS

In the analyses presented in this paper we restrict our attention to the case in which the initial fluctuations are adiabatic with a simple power-law spectrum; such perturbations are naturally produced in the standard single-field inflationary

model. Moreover, as is now common practice, we consider models in which the contents of the Universe are divided into three components: ordinary baryonic matter; cold dark matter (CDM), which interacts with baryonic matter solely through its gravitational effect; and an intrinsic vacuum energy. The present-day contributions of these components, measured as a fraction of the critical density required to make the Universe spatially flat, are denoted by Ω_b , Ω_{cdm} and Ω_Λ respectively. It is possible that some of the dark matter may, in fact, be in the form of relativistic neutrinos (hot dark matter), but the presence of a hot component has a negligible effect on the power spectrum, given the sensitivity and angular resolution of current CMB experiments (?). We therefore assume that all dark matter is cold and set $\Omega_\nu = 0$.

Following the current theoretical expectation (?), we also assume that the contribution of tensor mode perturbations is very small compared with the scalar fluctuations, and so we ignore their effects. This assumption is consistent with current observations. Since tensor modes contribute primarily to low multipoles, ℓ , the only existing measurement that would be particularly sensitive to their presence is the level of the CMB power spectrum at low- ℓ observed by the COBE-DMR experiment (?). If the tensor component made up a large fraction of this observed power, the value of the spectral index n_s for scalar perturbations would need to exceed unity by a considerable margin in order to provide the level of power at higher ℓ measured by numerous other CMB experiments. Such a large value of n_s is, however, ruled out by large-scale structure studies (?). Nevertheless, it must be remembered that this argument only holds if the initial perturbation spectrum is indeed a simple power-law.

Given the assumptions outlined above, there remain seven degrees of freedom in the description of the standard inflationary CDM model. The parameterisation of this seven-dimensional model space can be performed in numerous ways, but we shall adopt the most common choice, which is defined by the following parameters: the physical density of baryonic matter ($\Omega_b h^2 \equiv \omega_b$); the physical density of CDM ($\Omega_{\text{cdm}} h^2 \equiv \omega_{\text{cdm}}$); the vacuum energy density due to a cosmological constant (Ω_Λ); the total density (Ω_{tot}); the spectral index of the initial power-law spectrum of scalar perturbations (n_s); the optical depth to the last-scattering surface due to reionisation (τ); and the overall normalisation of the power spectrum as measured by $Q \equiv \sqrt{5C_2/(4\pi)}$ and is quoted relative to Q_{COBE} , as determined from the 4-year COBE-DMR data by ?. This choice of parameters is similar to that made in the analysis of the CMB band-power measurements obtained by the BOOMERanG, MAXIMA and DASI experiments. We note that, in this parameterisation, the reduced Hubble parameter h ($\equiv H_0 \text{ km s}^{-1} \text{ Mpc}^{-1}/100$) is auxiliary and is given by $h = \sqrt{(\omega_b + \omega_{\text{cdm}})/(\Omega_{\text{tot}} - \Omega_\Lambda)}$.

In comparing the observed CMB flat band-powers measured by the VSA with the above multidimensional model, we adopt a Bayesian approach based on the evaluation of the likelihood function for the data as a function of the cosmological parameters, which for brevity we denote by the vector $\theta = (\omega_b, \omega_{\text{cdm}}, \Omega_\Lambda, \Omega_{\text{tot}}, n_s, \tau, Q/Q_{\text{COBE}})$. To set proper constraints on the values of these parameters, it is necessary to explore the seven-dimensional model space over a region large enough to encompass those models with sig-

nificant likelihood. To that end, we employ two different techniques to explore the likelihood function: a traditional approach in which the likelihood function is evaluated on a grid of points in parameter space, and a Markov-Chain Monte Carlo (MCMC) technique in which a set of samples are drawn from the likelihood function. These techniques are described below. A common requirement of both methods, however, is the accurate evaluation of the likelihood function at any given point in the parameter space, and we begin by describing how this computation is performed.

2.1 Evaluation of the likelihood function

As described in Paper III, the constraints imposed by the VSA compact array observations on the CMB power spectrum have been obtained using the MADCOW analysis package (?). This provides a one-dimensional likelihood distribution for each flat band-power \mathcal{C}_B , conditioned on the values of the other band-powers at the joint maximum of the likelihood function. In addition the Hessian matrix at the joint maximum is also calculated, which may be inverted to obtain the elements $V_{BB'}$ of the covariance matrix of the flat band-power estimates under the assumption that the likelihood function is well approximated by a multivariate Gaussian near its peak.

Since the VSA measures power only on small angular scales ($\ell > 150$), it does not constrain the amplitude and tilt of the power spectrum at low- ℓ , which leads to pronounced degeneracies in the parameter space. Therefore, in Section 3, we also include in our analysis the 28 COBE-DMR band-powers provided in the RADPACK distribution (?). Moreover, in Section 4, we further include CMB band-power measurements obtained by the BOOMERanG, MAXIMA and DASI experiments.

In order to compare a set of observed flat band-powers $\mathcal{C}_{B,o}$ with our theoretical model, it is necessary to compute the corresponding predicted values $\mathcal{C}_{B,p}$ of these band-powers, given a particular set of parameter values θ . If \mathcal{C}_ℓ is the corresponding theoretical power spectrum for this set of parameter values, the predicted value of the B th flat band-power is given by

$$\mathcal{C}_{B,p} = \sum_{\ell} \frac{W_B(\ell)}{\ell} \mathcal{C}_\ell$$

where $\mathcal{C}_\ell = \ell(\ell+1)C_\ell/(2\pi)$ and $W_B(\ell)$ are the window functions for the experiment under consideration. The VSA window functions are presented in Paper III.

In the comparison of the observed and predicted band-powers it is necessary to take proper account of the uncertainties in our estimates of the $\mathcal{C}_{B,o}$. In fact, the uncertainties in band-power estimates are, in general, non-Gaussian and this precludes us from calculating a simple χ^2 -statistic. It is possible, however, to make a transformation from the flat band-powers to a related set of ‘offset log-normal’ variables for which the uncertainties are Gaussian to a very good approximation (?). This requires the calculation of an additional set of quantities x_B from the data, which represent the uncertainty due to instrumental noise. These are straightforwardly calculated for the VSA band-powers, and

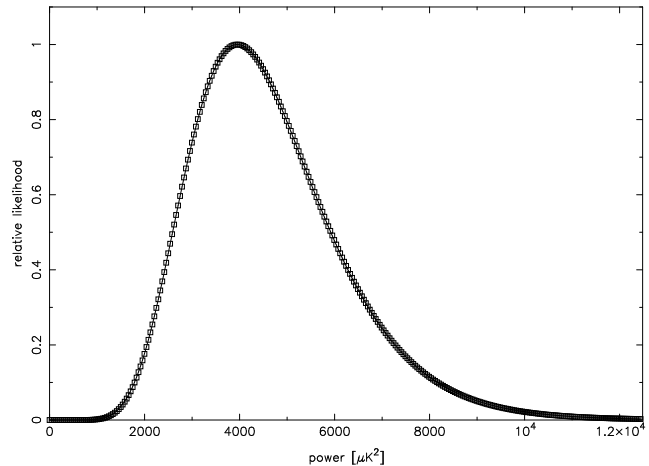


Figure 1. An example of true likelihood (points) and its offset log-normal approximation (line) for the flat band-power in the first VSA spectral bin for the combined data from the VSA1, VSA2 and VSA3 fields.

will be available on our web-site¹. The corresponding quantities for the DMR and DASI band-powers are included in the RADPACK package, and those for MAXIMA are available on their website. For BOOMERanG, however, the x_B values are not yet publicly available, and so we assume simply that the likelihood is a multivariate Gaussian.

The observed band-powers are then transformed as

$$\tilde{\mathcal{C}}_{B,o} = \ln(\mathcal{C}_{B,o} + x_B),$$

and similarly for the predicted band-powers. It is straightforward to show that the elements of the covariance matrix $\tilde{V}_{BB'}$ for the new variables are related to the covariance matrix $V_{BB'}$ of the original variables by

$$\tilde{V}_{BB'}^{-1} = (\mathcal{C}_{B,o} + x_B)(V)_{BB'}^{-1}(\mathcal{C}_{B',o} + x_{B'}).$$

The likelihood function is then taken to be a multivariate Gaussian in the transformed variables, so that

$$\mathcal{L}(\theta) \propto \exp(-\frac{1}{2}\chi^2),$$

where the χ^2 misfit statistic is given by

$$\chi^2 = \sum_{B,B'} (\tilde{\mathcal{C}}_{B,o} - \tilde{\mathcal{C}}_{B,p})(\tilde{V})_{BB'}^{-1}(\tilde{\mathcal{C}}_{B',o} - \tilde{\mathcal{C}}_{B',p}).$$

We find that this assumed form for the likelihood function provides an excellent fit to the true likelihood distribution for the VSA band-powers. This is illustrated in Fig. 1, in which we plot the true likelihood and the corresponding offset log-normal approximation for the flat band-power in the first VSA spectral bin for the combined data from the VSA1, VSA2 and VSA3 fields.

We note that the use of this transformation not only allows us to find the best-fit point in the parameter space θ , but also allows us to use the value of χ^2 at this point as a measure of goodness of fit.

¹ <http://www.mrao.cam.ac.uk/telescopes/vsa>

2.2 Exploration of the parameter space: grid-based approach

Once one has the facility to calculate accurately the likelihood function $\mathcal{L}(\theta)$ for the cosmological parameters θ at any given point in the parameter space, one must devise a strategy to explore the likelihood distribution throughout this space.

From the above discussion, it is clear that the evaluation of the likelihood function at each point in parameter space requires one to calculate the theoretical power spectrum corresponding to that point. The calculation of this C_ℓ spectrum is performed using version 4.0 of the CMBFAST code (?), which uses a k -space splitting technique that accelerates the calculation of the spectrum by using a flat $\Omega_{\text{tot}} = 1$ model to compute the high- ℓ multipoles for models with $\Omega_{\text{tot}} \neq 1$. Nevertheless, the calculation of a typical spectrum for a $\Omega_{\text{tot}} \neq 1$ model still requires around 30 sec of CPU time on one of the processors of the COSMOS SGI Origin 2000 computer. Even with the 16 processors available to us, this computational cost severely limits the total number of points in parameter space at which the likelihood function can reasonably be evaluated. We note that, in fact, two complete grids of models (and two independent pipelines for the cosmological parameters estimation) were set up in Tenerife and Cambridge.

The traditional approach is thus to calculate the C_ℓ spectra for a grid of models that is as fine as CPU-time limitations allows, while being sufficiently large to encompass the entire probability distribution. For our model space, we calculated C_ℓ spectra on a six-dimensional grid corresponding to the values for each parameter given in Table 1. The six-dimensional grid contains 419 968 spectra. Since the different values of the scalar spectral index n_s can all be obtained on a single call to CMBFAST, this required 52 496 runs in total and took ~ 2 days of CPU time on COSMOS. The overall normalisation parameter Q/Q_{COBE} need not be pre-computed on a grid since it produces a simple linear scaling of the C_ℓ spectra. In this parameter, the likelihood function was calculated at 10 points in the range 0.45 to 1.44, with a step size of 0.11.

The likelihood function $\mathcal{L}(\theta)$ for a given dataset can be evaluated at each of these grid points as described in section 2.1, and the location of the maximum determined. For each cosmological parameter, the one-dimensional marginalised distribution is then obtained by numerically integrating over the other parameters. These marginal distributions are then interpolated with a cubic spline, and determine the constraints placed on the cosmological parameters.

Wherever possible, we also include the calibration uncertainties of the CMB experiments under consideration as extra parameters in our analysis. The prior on such parameters is taken as a Gaussian centred on unity, with a standard deviation of the appropriate width. An analytic marginalisation is performed over this parameter, using the method proposed by ?. This analytical procedure assumes, in addition to a Gaussian prior on the calibration parameter, that the likelihood function is Gaussian. Unfortunately, in neither the original band-powers, nor the offset log-normal variables, are *both* these functions precisely Gaussian, and so some (small) approximation is introduced. In this paper, the analytical

marginalisation is performed before transforming to offset log-normal variables.

2.3 Exploration of the parameter space: MCMC approach

In a parameter space of large dimensionality, a natural alternative to the grid-based approach is instead to sample from the likelihood distribution. An efficient procedure for obtaining such samples is to construct a Markov chain whose equilibrium distribution corresponds to the likelihood function in parameter space (see e.g. ?). Thus after propagating the Markov chain for a given ‘burn-in’ period, one obtains samples from the likelihood distribution, provided the chain has converged.

The MCMC sampling procedure may be implemented most straightforwardly by using a simplified version of the Metropolis–Hastings algorithm. At each step n in the chain, the next state θ_{n+1} is chosen by first sampling a candidate point θ' from some proposal distribution $\pi(\theta)$. The candidate point is then accepted with probability

$$\alpha = \min \left[1, \frac{\pi(\theta_n)\mathcal{P}(\theta_{n+1})}{\pi(\theta_{n+1})\mathcal{P}(\theta_n)} \right].$$

where $\mathcal{P}(\theta)$ is the posterior distribution for the parameters θ and is simply the product of the likelihood $\mathcal{L}(\theta)$ and some prior $p(\theta)$; we take the latter to be uniform unless otherwise stated. If the candidate point is accepted, the next state in the chain becomes $\theta_{n+1} = \theta'$, but if the candidate point is rejected, the chain does not move, and $\theta_{n+1} = \theta_n$. In theory, the convergence of the chain to the limiting distribution is independent of the choice of the proposal distribution but this choice is crucial in determining both the rate of convergence to the limiting distribution and the efficiency of the subsequent sampling. An effective approach is to set the proposal distribution $\pi(\theta)$ to a multivariate Gaussian, centred on the current point in parameter space.

As mentioned above, the states of the chain θ_n can be regarded as samples from the limiting (i.e. likelihood) distribution only after some initial burn-in period for the chain to reach equilibrium. The topic of convergence is still a matter of statistical research and no definitive formula exists for calculating the required length of the burn-in period. Nevertheless, several convergence diagnostics have been proposed (?), which may be used as a guide.

After burn-in, the sample density is directly proportional to the likelihood distribution, and so the samples may be used straightforwardly to obtain estimates of the parameter values and confidence limits. In particular, one may easily obtain one-dimensional marginalised distributions for each parameter separately, obviating the need for computer-intensive numerical integrations. Moreover, the computational requirements of MCMC procedures are almost independent of dimensionality of parameter space and thus allow a large number of parameters to be constrained simultaneously by the data.

The strength of MCMC methods lies in the fact that useful parameter estimations can be achieved with considerably fewer likelihood evaluations as compared to the traditional grid-based methods. Nevertheless, the density of samples must be high enough so that the estimation of the underlying posterior probability distribution is not plagued by

Table 1. The values of the parameters in the six dimensional grid of models.

$\Omega_b h^2$:	0.010	0.015	0.020	0.025	0.030	0.035	0.040	0.045	0.050				
$\Omega_{\text{cdm}} h^2$:	0.02	0.06	0.1	0.2	0.3	0.4	0.5	0.6	0.7	0.8	0.9	1.0	1.1
Ω_Λ :	0.0	0.1	0.2	0.3	0.4	0.5	0.6	0.7	0.8				
Ω_{tot} :	0.7	0.75	0.80	0.85	0.90	1.00	1.05	1.10	1.15	1.20	1.30		
n_s :	0.7	0.8	0.9	1.0	1.1	1.2	1.3	1.4					
τ :	0.0	0.025	0.05	0.075	0.1	0.2	0.3	0.5					

Poisson noise and is independent of the kernel density estimation method. Usually one requires on the order of several tens of thousands of (accepted) samples. The efficiency with which these samples may be obtained depends strongly on the shape of the posterior likelihood function and in practice the basic Metropolis–Hastings algorithm can be augmented by the use of various speed-ups. Most notably, the sampling efficiency is improved by considering several simultaneous correlated Markov chains and by specific random point generators that attempt to follow the shape of the likelihood distribution posterior. The main MCMC implementation used here is that provided by the BAYESYS software (Skilling, private communication), which employs several enhancements of the basic Metropolis–Hastings algorithm and has the ability to sample using multiple chains.

Ideally, one would like to calculate a theoretical power spectrum using one of the popular packages, such as CAMB or CMBFAST for each sample. However, this is computationally extremely expensive. As a practical alternative, one can use a pre-computed grid of theoretical spectra, such as that discussed in section 2.2, and calculate the required spectrum by suitable interpolation between neighbouring grid points. The density of grid points in the parameter space must be small enough that the dominant error in the estimated cosmological parameters comes from the errors in the measured CMB power spectrum and not from the interpolation between the grid points. We tested the accuracy of the grid discussed in section 2.2 by calculating the exact CMB power spectrum using CMBFAST for 1000 randomly chosen sets of parameters and comparing them with grid interpolation. We find that the rms error on the predicted band-powers resulting from the interpolation is around 4 per cent, which is very small as compared with the uncertainties in the band-powers from the current CMB experiments.

The BAYESYS sampler provides a powerful general purpose MCMC engine, which allows one to explore complicated likelihood functions of large dimensionality. We find, however, that the present accuracy of the CMB experiments results in likelihood surfaces that are relatively smooth and highly convex, which can be adequately explored using a simple MCMC sampler based solely on the straightforward Metropolis–Hastings algorithm. This allows the possibility of tailoring an MCMC algorithm to the specific problem of cosmological parameter estimation from CMB band-power measurements, and taking advantage of our prior knowledge concerning which parameter combinations can be calculated quickly using CMBFAST or CAMB and which directions in parameter space to avoid. Such an approach has been implemented in the software package COSMOMC (?), and allows one to perform an MCMC exploration of the parameter space in which the use of a grid is bypassed altogether,

and the exact theoretical C_ℓ spectrum is calculated at each sample point. We have made use of this approach as an additional cross-check of our results.

In addition to using the MCMC approach to provide useful checks of the parameter constraints obtained from the standard grid-based method, we have exploited the insensitivity of the MCMC method to the dimensionality of the problem by including calibration uncertainty in our numerical analysis, rather than performing an approximate analytical marginalisation over it, as performed in the grid-based approach. A new parameter a is introduced which is the ratio of the *real* telescope calibration to the experimental best estimate. A Gaussian prior is assumed for a , with its centre at unity and with a standard deviation corresponding to the calibration uncertainty of the experiment under consideration. Whenever the MCMC algorithm requires a sample for a given value of a , the data are rescaled accordingly.

3 COSMOLOGICAL PARAMETER CONSTRAINTS FROM THE VSA

We first consider the constraints placed on the values of the cosmological parameters $\theta = (\omega_b, \omega_{\text{cdm}}, \Omega_\Lambda, \Omega_{\text{tot}}, n_s, \tau, Q/Q_{\text{COBE}})$ using only the VSA band-powers, and the low- ℓ normalisation provided by the 28 COBE-DMR band-powers provided in the RADPACK package. The precise VSA data used were the 10 band-power estimates and associated covariance matrices for each of the three separate 3-field mosaics VSA1, VSA2 and VSA3.

3.1 Grid-based approach

Using the approach outlined in section 2.2, we calculate the corresponding likelihood function $\mathcal{L}(\theta)$ over the six-dimensional grid summarised in Table 2 and the normalisation parameter Q/Q_{COBE} . In addition, we include the calibration uncertainty of the VSA band-powers as an extra parameter in our analysis. The prior on this parameter is taken as a Gaussian centred on unity, with a standard deviation corresponding to the known calibration error for the VSA of 7 per cent in $(\Delta T)^2$.

After analytically marginalising over calibration uncertainty, the best-fit model is characterised by the parameter values $(\omega_b, \omega_{\text{cdm}}, \Omega_\Lambda, \Omega_{\text{tot}}, n_s, \tau, Q/Q_{\text{COBE}}) = (0.020, 0.06, 0.7, 1.0, 0.9, 0.0, 0.87)$, but no particular significance should be attached to this model. It is the marginalised constraints on the individual parameters that are most important. Nevertheless, it is of interest to determine the goodness-of-fit for this model. At the peak, the value of χ^2 was found to be 47.3 for the 3×10 VSA plus 28

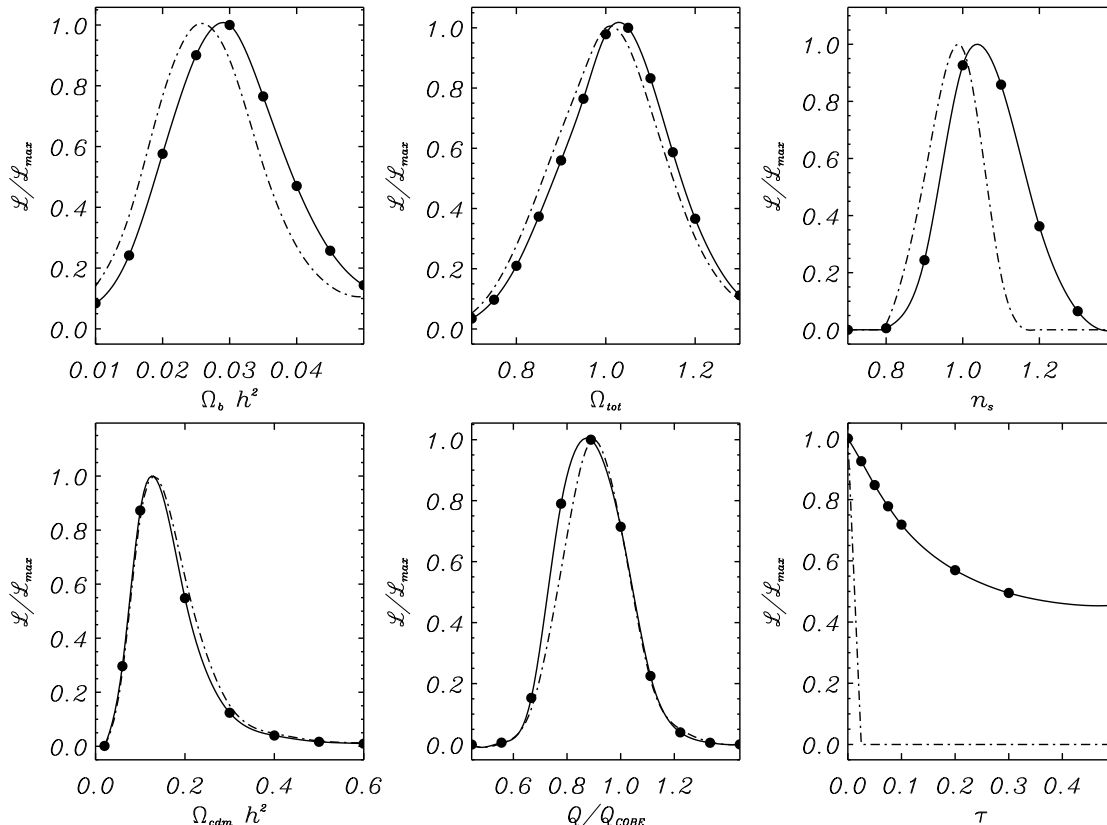


Figure 2. Marginalised distributions for the cosmological parameters as determined from the VSA experiment, together with a normalisation constraint at low- ℓ from COBE-DMR. The solid lines include the effect of a weak top-hat prior on h ($0.4 < h < 0.9$) and an implicit top-hat prior on τ ($0 < \tau < 0.5$) resulting from the grid boundaries. The dot-dashed lines correspond to the additional prior $\tau = 0$. The lines are constructed using a cubic spline interpolation through the grid points, which are shown as solid circles.

Table 2. Cosmological parameters estimated from VSA and COBE-DMR data, using several priors. It should be noted that these estimates include the effect of the implicit priors on the parameters resulting from the finite grid of models (see Table 1). All the confidence regions correspond to the 68 per cent level.

Prior	$\Omega_b h^2$	n_s	Ω_{tot}	$\Omega_{cdm} h^2$	Ω_m	Ω_Λ
$\{0.4 < h < 0.9\}$	$0.029^{+0.009}_{-0.009}$	$1.04^{+0.11}_{-0.08}$	$1.03^{+0.12}_{-0.12}$	$0.13^{+0.08}_{-0.05}$	-	-
$\{0.4 < h < 0.9\} + \{\tau = 0\}$	$0.026^{+0.008}_{-0.008}$	$0.99^{+0.06}_{-0.07}$	$1.01^{+0.12}_{-0.13}$	$0.13^{+0.08}_{-0.05}$	-	-
$\{10 \text{ Gyr} < \text{age} < 20 \text{ Gyr}\}$	$0.028^{+0.009}_{-0.008}$	$1.02^{+0.11}_{-0.08}$	$1.05^{+0.14}_{-0.12}$	$0.12^{+0.05}_{-0.04}$	-	-
$\{10 \text{ Gyr} < \text{age} < 20 \text{ Gyr}\} + \{\tau = 0\}$	$0.025^{+0.008}_{-0.008}$	$0.97^{+0.06}_{-0.07}$	$1.03^{+0.15}_{-0.12}$	$0.12^{+0.06}_{-0.04}$	-	-
$\{h = 0.72 \pm 0.08\} + \{10 \text{ Gyr} < \text{age} < 20 \text{ Gyr}\}$	$0.028^{+0.007}_{-0.008}$	$1.00^{+0.06}_{-0.05}$	$0.96^{+0.06}_{-0.12}$	$0.19^{+0.08}_{-0.07}$	$0.48^{+0.08}_{-0.21}$	$0.47^{+0.33}_{-0.16}$
$\{\text{SNIa}\} + \{0.4 < h < 0.9\}$	$0.029^{+0.009}_{-0.009}$	$1.02^{+0.12}_{-0.08}$	$1.02^{+0.08}_{-0.06}$	$0.09^{+0.05}_{-0.04}$	$0.32^{+0.09}_{-0.06}$	$0.71^{+0.07}_{-0.07}$

COBE-DMR band-powers. Assuming that a full 7 degrees of freedom are lost to the fit (which is unlikely given the form of the theoretical power spectra), we thus have 51 remaining degrees of freedom. The value $\chi^2_{51} = 47.3$ lies at the 38 per cent point on the χ^2_{51} cumulative distribution function, which is entirely acceptable and shows that model to be a good fit to the data.

For a multidimensional likelihood function calculated on a grid, one has already implicitly assumed top-hat priors on each of the parameters, corresponding to the edges of the grid. It should also be borne in mind that, in principle, if the grid does not encompass all of the likelihood in *any* parameter, then that top-hat prior becomes relevant for *all* of

the parameters. In addition to the implicit prior arising from the grid, we may also impose explicit priors on the cosmological parameters values, according to our existing knowledge (or prejudices) concerning their values. In particular, we consider combinations of the following five priors: (i) a weak top-hat prior on h ($0.4 < h < 0.9$); (ii) a strong prior Gaussian on h ($h = 0.72 \pm 0.08$, ?); (iii) a weak top-hat prior on age ($10 \text{ Gyr} < t < 20 \text{ Gyr}$); (iv) a strong prior on optical depth ($\tau = 0$); (v) a prior in the $(\Omega_m, \Omega_\Lambda)$ -plane from high-redshift Type IA supernovae (where $\Omega_m = \Omega_b + \Omega_{cdm}$) (?). After adopting (combinations of) these priors, we then obtain the one-dimensional marginalised distribution for each cosmological parameter by direct numerical integration; the

successive integrals over the parameter directions are evaluated in turn by first performing a cubic spline interpolation onto a fine regularly-space grid of points.

An illustration of our results is shown in Fig. 2 for the two cases in which we assume prior (i) above on h , with and without the additional prior (iv) on τ . The solid lines represent results treating τ as a free parameter, whereas the dot-dashed lines correspond to setting $\tau = 0$. It is clear from the figure that the effect of this latter prior is minimal, leading only to minor changes in the constraints on $\Omega_b h^2$ and n_s , which is to be expected from the well-known degeneracy between these two parameters (?).

The 68 per cent confidence limits derived from these marginal distributions on the cosmological parameters ω_b , ω_{cdm} , Ω_{tot} and n_s are given in the first two rows of Table 2. The upper and lower limit in each case is defined such that the corresponding interval contains 68 per cent of the total probability, and the likelihood function evaluated at each limit has the same value; the quoted best-fit value is the mode of the corresponding marginalised distribution. Also listed in the table are the 68 per cent confidence limits on these parameters resulting from (combinations of) the different priors listed above. We note that the constraints on these four parameters are relatively insensitive to the inclusion of increasingly stringent priors. In particular, we see that the constraints on ω_b are all consistent with the constraint $\omega_b = 0.020 \pm 0.002$ (95%) (?) resulting from the observed primordial hydrogen-deuterium ratio and the theory of nucleosynthesis. Depending on the prior assumed, the preferred value of ω_{cdm} is typically around 0.12, with an uncertainty of 0.05, and lends very strong support to existing evidence for the existence of non-baryonic dark matter. We also note that, for all the priors considered, the constraints on the total density Ω_{tot} are consistent with the Universe being spatially flat. Finally, and again independently of the particular prior assumed, the constraints on the scalar spectral index are consistent with the scale-invariant $n_s = 1$ (Harrison–Zel’dovich) initial power spectrum, which is preferred by standard inflationary models.

In the first four rows of Table 2, the priors are unable to break the well-known degeneracy of CMB data in the $(\Omega_m, \Omega_\Lambda)$ -plane, and so no constraints are given. Nevertheless, with the assumption of our strong prior on h and a weak prior on the age of the Universe, we see that one begins to break this degeneracy. Indeed, one finds that the preferred values of Ω_m and Ω_Λ correspond to a roughly equal partitioning of the critical density between matter (baryonic and dark) and vacuum energy, although the lower limit for Ω_m and the upper limit for Ω_Λ extend some way from the best-fit values. Finally, the assumption of the high-redshift SNIa constraint (?) and our weak prior on h , succeed in cleanly breaking the CMB degeneracy and we find the partitioning of the critical density between matter and vacuum energy is well constrained in the approximate proportions one-third to two-thirds.

3.2 MCMC approach

Using precisely the same data as analysed in the previous section, we also explored the seven-dimensional parameter space θ using the MCMC techniques outline in section 2.3. First, we used the BAYESYS algorithm and, for each sam-

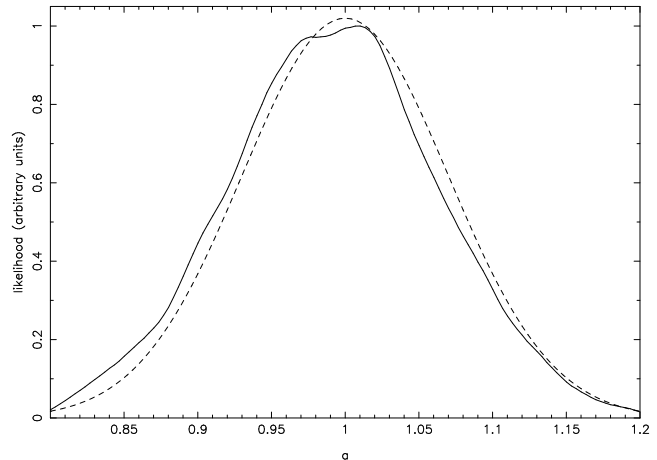


Figure 3. The marginalised distribution for the calibration parameter a after analysing the data (solid line). Also plotted is the original prior placed on a (dashed line).

ple, calculated the theoretical C_ℓ spectrum by interpolating from the pre-computed grid. Since the shape of the likelihood function is very simple, it was enough to run just eight simultaneous Markov chains, with each walk requiring only a very short burn-in period. After burn-in, we collected 3000 samples from each chain, thus obtaining 24000 samples in total from the likelihood distribution. As one would hope, we find that all parameter constraints calculated from these samples are fully consistent with those obtained above for each set of imposed priors. We therefore do not reproduce them here, although they do provide a useful check on our earlier results.

As mentioned in section 2.3, to illustrate the flexibility of the MCMC approach, we included the calibration uncertainty of the VSA band-power measurements as an additional parameter in our numerical analysis. The prior on this parameter a was taken to be a Gaussian centred at unity, with standard deviation 0.07. In Fig. 3, we plot this prior distribution, together with the marginalised distribution on the parameter a after analysing the data. The mean of this distribution lies at $a = 1.00$ and has a standard deviation of 0.071. Thus, we see that, within the class of models considered, the measured CMB band-powers are consistent with our estimated calibration uncertainty.

As a second illustration of the usefulness of the MCMC approach, we plot in Fig. 4 a novel representation of the sets of cosmological models consistent with the VSA plus COBE-DMR data, which is produced as follows. Each of the MCMC samples corresponds to a theoretical C_ℓ spectrum. Thus from the samples it is straightforward to construct a one-dimensional distribution of the power at each multipole ℓ . In Fig. 4, the position of the maximum of the distribution at each ℓ is shown by the solid line, while the dashed and dot-dashed lines indicate the 68 and 95 per cent confidence limits of the distribution respectively, determined in the same manner as in section 3.1. This plot assumes our earlier weak prior on the age of the Universe. We note that the first peak is very well defined, and that there is also good evidence for the second peak.

As mentioned in section 2.3, we also check our cosmological parameter constraints by using the straightforward

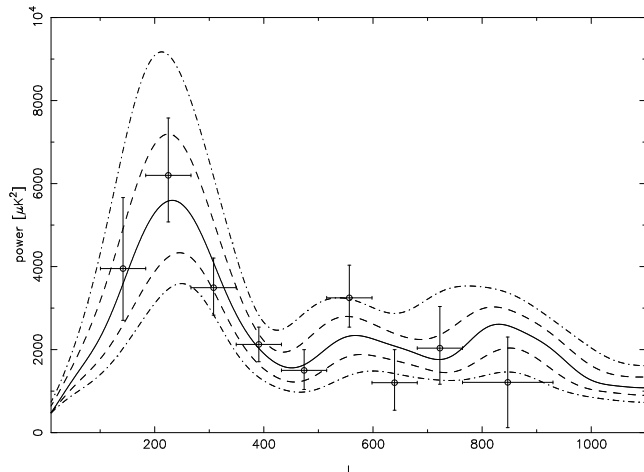


Figure 4. An illustration of the MCMC sample density on the (l, C_l) -plane. The solid line represents the maximum of the sample density at a given l -value, while dashed and dot-dashed lines correspond to 68 per cent and 95 per cent confidence limits. The vertical lines are VSA data points with 68 per cent confidence limits. Note that samples were obtained using full covariance information, which cannot be displayed conveniently on a single plot.

COSMOMC algorithm, which is optimised for the problem at hand and bypasses the need for a grid. Once again our results are fully consistent with those found above, and provide another useful check on our analysis.

4 COMBINING VSA WITH OTHER CMB EXPERIMENTS

So far we have only combined the VSA data with the COBE-DMR experiment in order to place limits on cosmological parameters from the CMB. It is clear, however, that tighter constraints may be obtained if we additionally include information from other CMB experiments, in particular BOOMERanG (?), DASI (?), and MAXIMA (?).

In Fig. 5, we begin by simply plotting the maximum-likelihood estimates for $\Omega_b h^2$, Ω_{tot} , n_s and $\Omega_{cdm} h^2$ obtained by the VSA and these other recent CMB experiments, together with the reported 68 per cent confidence intervals (except for MAXIMA, for which we plot as error bars 1/2 of the reported 95 per cent confidence limits). We note that the confidence limits for each experiment include the effects of calibration and beam uncertainty, where appropriate, and each experiment also assumes the COBE-DMR band-powers and similar weak priors to those adopted in section 3.1.

In general, the constraints on each individual parameter agree within error bars. Moreover, since each of these experiments uses different observing techniques and has observed different regions of the sky, we may consider each measurement as an independent estimate of the corresponding parameter. Assuming further that the individual likelihoods are Gaussian, they may be immediately combined to produce a joint constraint on each parameter, which is also shown in the figure.

In the top panel, corresponding to the parameter $\Omega_b h^2$, we also plot the 68 per cent confidence limits arising from the nucleosynthesis constraint $\Omega_b h^2 = 0.020 \pm 0.001$ (?).

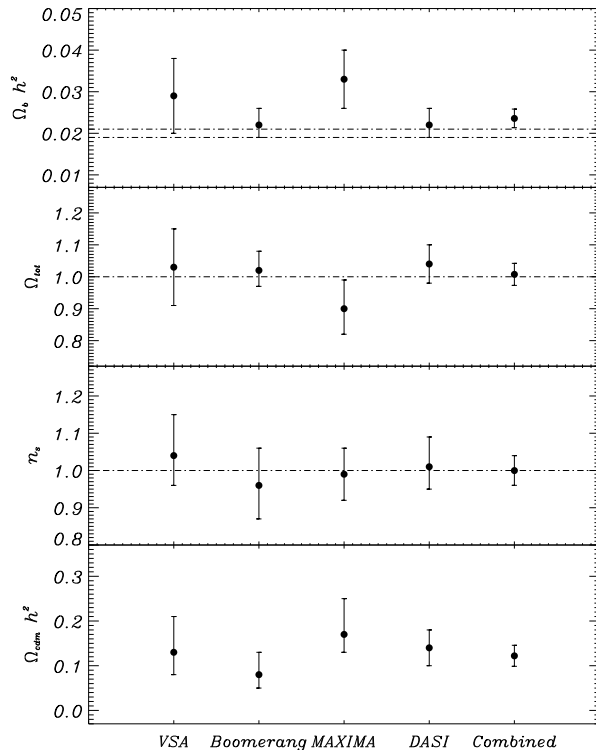


Figure 5. Comparison of the maximum likelihood estimates and 68 per cent confidence limits on the cosmological parameters $\Omega_b h^2$, Ω_{tot} and n_s from the VSA and recent other CMB experiments (see text).

The combined measurement from all CMB experiments is consistent with the BBN constraint and fully supports the case for a low value of the primordial deuterium abundance. It also favours a primordial helium mass fraction of $Y_p \approx 0.246$. In the second panel, we see that all the experiments agree with the prediction $\Omega_{tot} = 1$ of standard inflationary models. Remarkably, the combined CMB measurement has an error bar of only ~ 3 per cent. The combined value for n_s also agrees at the $1\text{-}\sigma$ level with the scale-invariant Harrison-Zel'dovich initial power spectrum, i.e. with $n_s = 1$. Finally, we see that the combined value $\Omega_{cdm} h^2$ is tightly constrained to be around 5 times larger than the value for $\Omega_b h^2$, which is a strong indication for the existence of non-baryonic matter.

In Fig. 6 we compare the VSA+SNIa constraints on Ω_m and Ω_Λ , with those published by the other recent CMB experiments. It is important to note, however, that the published DASI value does not make use of any SNIa data, so in order to enable a proper comparison to be made, we have repeated the complete grid-based parameter estimation procedure for DASI performed by ?, using their published covariance matrices and window functions, but including the SNIa prior from ? and a weak prior on h . Incidentally, we found that the parameter constraints we derived for DASI before including the SNIa prior were in complete agreement with those obtained by ?. In Fig. 6, we plot the 68 per

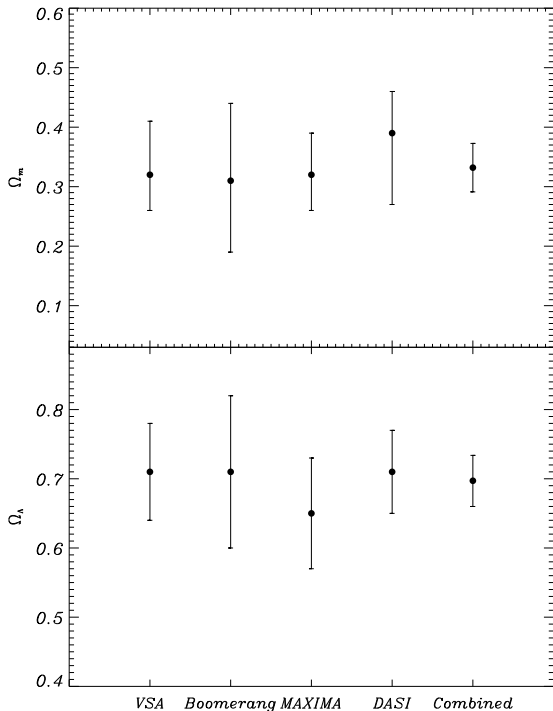


Figure 6. Comparison of the maximum likelihood estimates for Ω_m and Ω_Λ from the VSA and recent CMB experiments. A prior from SNIa measurements is adopted (Perlmutter et al. 1999), as well as a weak prior on H_0 .

cent confidence limits from each experiment, and we see that they are all in good agreement. The combined constraint is $\Omega_m = 0.33^{+0.04}_{-0.04}$ and $\Omega_\Lambda = 0.70^{+0.04}_{-0.04}$.

As noted previously by ?, by combining all the available CMB datasets together with a strong prior on h , it is possible to break cleanly the CMB degeneracy in the $(\Omega_m, \Omega_\Lambda)$ -plane *without* using the SNIa prior. As our CMB datasets, we use the VSA and COBE-DMR band-powers, the RADPACK compilation for DASI, plus the published results from BOOMERanG and MAXIMA. By performing a simple grid-based parameter estimation procedure, as outlined in section 2.2, we find that one can break the $(\Omega_m, \Omega_\Lambda)$ -plane CMB degeneracy by assuming only our weak prior on the age of the Universe ($10 \text{ Gyr} < \text{age} < 20 \text{ Gyr}$) and our strong Gaussian prior on h ($h = 0.72 \pm 0.08$) from the HST key project. Our resulting constraints are $\Omega_m = 0.28^{+0.14}_{-0.07}$ and $\Omega_\Lambda = 0.72^{+0.07}_{-0.13}$, which are similar to those derived above, but are independent of the SNIa data. Hence, this result is not subject to the usual uncertainties associated with using high-redshift type IA supernovae as standard candles. We stress that a very similar result would be obtained by instead combining the CMB data with the prior on h from Sunyaev–Zel’dovich and X-ray observations of clusters (?).

5 DISCUSSION

In Figs 5 and 6 we have presented results of cosmological parameter extraction from various CMB experiments. These experiments use a variety of observational techniques and operate at a range of frequencies and have therefore widely different systematic effects. Nevertheless, the figures show remarkable agreement between different experiments. This may indicate the importance of the assumed weak priors (which are often common) and possibly the fitting of too many parameters given the constraining power of individual experiments. Indeed, the reduced χ^2 is below 1 for most experiments (see individual papers). Nevertheless, when one combines experiments (VSA, DASI, BOOMERanG, MAXIMA and DMR data) most cosmological parameters become constrained at the level ranging between 5–20 per cent, if one neglects the possibility of tensor modes. This accuracy rivals the discriminatory power of the upcoming CMB satellite experiments, such as MAP (?), with the added bonus that the residual systematic effects of the various experiments are diluted.

We also verify that a constraint on the vacuum energy component of the Universe may be obtained *independently* of the Type Ia supernovae data, by combining the results from CMB experiments alone, together with the a prior on h from the HST key project (?). Moreover, the resulting values for Ω_Λ and Ω_m are consistent with those obtained when supernovae data are included. It is often assumed that CMB experiments cannot constrain the vacuum energy, as a result of the well known CMB degeneracy in the $(\Omega_m, \Omega_\Lambda)$ -plane, and the SNIa data are usually employed to break this degeneracy. The supernovae data are, however, still somewhat plagued by uncertain systematic effects (such as extinction along the line of sight and the evolutionary effects due to metallicity), although the issues are gradually being resolved (?). Therefore, obtaining independent consistent results on the value of the cosmological constant increases our confidence in both the supernovae and CMB results.

6 CONCLUSIONS

In our analysis of the newly available data from the VSA compact array, and other recent cosmological results, we have found the following.

- Traditional grid-based methods and Markov-Chain Monte Carlo (MCMC) sampling techniques have been applied to the cosmological parameter estimation problem and found to yield consistent results.
- The VSA observations, when combined with the COBE-DMR data and a weak top-hat prior on h ($0.4 < h < 0.9$) give $\Omega_{\text{tot}} = 1.03^{+0.12}_{-0.12}$, $\Omega_b h^2 = 0.029^{+0.009}_{-0.009}$, $\Omega_{\text{cdm}} h^2 = 0.13^{+0.08}_{-0.05}$ and $n_s = 1.04^{+0.11}_{-0.08}$ at the 68 per cent confidence level.
- Adding in observations of type Ia supernovae, the CMB degeneracy in the $(\Omega_m, \Omega_\Lambda)$ -plane may be broken to yield the constraints $\Omega_m = 0.32^{+0.09}_{-0.06}$ and $\Omega_\Lambda = 0.71^{+0.07}_{-0.07}$.
- The BOOMERanG, DASI and MAXIMA experiments, which have different approaches and systematics, yield consistent constraints on cosmological parameters, which is gratifying. Combining the results of these recent CMB experiments with the VSA data, and assuming weak priors

on h and the age of the Universe, gives $\Omega_{\text{tot}} = 1.01_{-0.03}^{+0.03}$, $\Omega_{\text{b}}h^2 = 0.024_{-0.002}^{+0.002}$, $\Omega_{\text{cdm}}h^2 = 0.12_{-0.02}^{+0.02}$ and $n_{\text{s}} = 1.00_{-0.04}^{+0.04}$.

- Adding in the type Ia supernovae constraint to the combined CMB result, the $(\Omega_{\text{m}}, \Omega_{\Lambda})$ -plane degeneracy is cleanly broken to give $\Omega_{\text{m}} = 0.33_{-0.04}^{+0.04}$ and $\Omega_{\Lambda} = 0.70_{-0.04}^{+0.04}$.

- One can equally well break the $(\Omega_{\text{m}}, \Omega_{\Lambda})$ -plane degeneracy without the SNIa data, by assuming the strong prior on h from either the HST Key Project or Sunyaev–Zel’dovich and X-ray observations of clusters. This yields the constraints $\Omega_{\text{m}} = 0.28_{-0.07}^{+0.14}$ and $\Omega_{\Lambda} = 0.72_{-0.13}^{+0.07}$.

ACKNOWLEDGEMENTS

We thank Sarah Bridle for providing her grid-based likelihood programs, Antony Lewis for making available his COSMOMC code and John Skilling for allowing us to use his BAYESYS MCMC sampler. This research was conducted in cooperation with SGI utilising the HEFCE-supported COSMOS supercomputer. We also acknowledge the IAC Computer Centre for helping with the setup of a 10-processor Beowulf system dedicated to this research. We thank the staff of the Mullard Radio Astronomy Observatory, Jodrell Bank Observatory and the Teide Observatory for invaluable assistance in the commissioning and operation of the VSA. The VSA is supported by PPARC and the IAC. Partial financial support was provided by the Spanish Ministry of Science and Technology project AYA2001-1657. A. Taylor, R. Savage, B. Rusholme and C. Dickinson acknowledge support by PPARC studentships. K. Cleary and J.A. Rubiño-Martin acknowledge Marie Curie Fellowships of the European Community programme EARASTARGAL, ‘The Evolution of Stars and Galaxies’, under contract HPMT-CT-2000-00132. K. Masinger acknowledges a Marie Curie Fellowship of the European Community. A. Slosar acknowledges the support of St. Johns College, Cambridge. We thank Professor Jasper Wall for assistance and advice throughout the project.

This paper has been typeset from a $\text{\TeX}/\text{\LaTeX}$ file prepared by the author.